crystals

MDPI

Article

Development of the Forming Limit Diagram for AA6016-T4 at Room Temperature Using Uniaxial Tension of Notched Samples and a Biaxial Test

Ahmed Elsayed *, Diego Gonzalez and Evgenia Yakushina

Advanced Forming Research Centre, Strathclyde University, Glasgow PA4 9LJ, UK; diego.gonzalez@strath.ac.uk (D.G.); evgenia.yakushina@strath.ac.uk (E.Y.)
* Correspondence: ahmed.elsayed@strath.ac.uk

Abstract: Within the framework of the formability limit assessment in sheet metal forming, testing of notched tensile samples coupled with digital image correlation (DIC) has been analysed as an alternative to overcome the implications of Nakajima testing in relation to times of test preparation, cost of the equipment, presence of friction, and amount of material required for the test. Additionally, the complications of the Nakajima testing at elevated temperatures need to also be considered. In this work, specific notched sample geometries have been investigated to accurately identify the forming limits of Aluminium alloy AA6016 in T4 condition. Once the notched geometry had been defined, experimental tensile testing of the samples coupled with DIC technology allowed us to identify the formability limits of interest. Finally, a comparison at room temperature with the conventional Nakajima testing was performed experimentally. Two different methodologies for strain limit evaluation in notched samples have been investigated in the present analysis. The first one is called a position-dependent method and is based on the inverse best-fit parabola of the "bell-shaped curve", which is used in the conventional Nakajima test. The second approach referred to a time-dependent method and is based on the strain rate evaluation at the necking zone. This strain-rate-dependent method, which works in combination with DIC measurements, was found to be more accurate to determine the necking limits than the previous one; in addition, it also provides more accurate information for the safe zone of forming.

Keywords: forming limit diagram; Nakajima test; notched samples; formability; position-dependent method; time-dependent method; digital image correlation; AA6016-T4

Citation: Elsayed, A.; Gonzalez, D.; Yakushina, E. Development of the Forming Limit Diagram for AA6016-T4 at Room Temperature Using Uniaxial Tension of Notched Samples and a Biaxial Test. *Crystals* **2023**, *13*, 1134. https://doi.org/10.3390/cryst13071134

Academic Editor: Umberto Prisco

Received: 8 June 2023
Revised: 26 June 2023
Accepted: 4 July 2023
Published: 20 July 2023

1. Introduction

When designing a sheet metal forming manufacturing process, material formability is a critical aspect. The formability of metals is influenced by many different factors, including the temperature, the strain rate, the microstructure of the metal, the sheet thickness, the strain path followed during forming, and the as-received material condition (linked to the microstructure, as previously mentioned) [1,2]. Any assistance for the engineers dealing with the formability assessment at the process design stage becomes unevaluable.

The forming limit diagram (FLD) is a graphical representation of the limits of the amount of deformation that sheet metal can undergo under different strain states during the forming process before failure. It is a critical tool used by the sheet metal forming industry and its concept firstly was introduced by Keeler and Goodwin [3]. The development of the FLD measuring from the 1960s was around two main points. First is how to measure the strain of the deformed sheet; second is how to define the forming limit of the material.

In 1968, Keeler [4] proposed the curricular grid system to measure the direction and magnitude of the strain, while Goodwin [5] experimentally demonstrated this approach. After that, other researchers proposed different types of grids to measure the strain. For

example, in 1982, Sowerby et al. [6] proposed a quadrilateral pattern for strain measurements. Later, Tan et al., (1992) [7] proposed the image processing technique to measure accurately the surface strain from the grids instead of the manual approach. In 1999, the spackle pattern was used by Vacher et al. [8] with a single camera to measure the strain. Finally, the digital image correlation technique has been developed and is currently used to track the change in the surface strain during the test [9].

Traditionally, the Nakajima test has been widely used to determine the formability limits of sheet metals. This type of test involves deforming different blank geometries using a hemispherical punch until fracture. By altering the width of the gauge section of the blank, different stretch-forming conditions are induced on the sheet metal surface, ranging from regular biaxial deformation to a simple tensile load [2]. Currently, the test is performed with DIC using a position-dependent method to define the necking limit.

However, the Nakajima test requires the use of expensive equipment and is considered a time- and resource-consuming methodology; moreover, friction is a common issue in this test since it affects the accuracy of the crack location. In addition, the implementation of the Nakajima test at elevated temperatures can be challenging, especially when it comes to capturing the strain data [10,11].

As an alternative approach, notched tensile samples have been introduced to overcome the limitations of Nakajima testing [12]. The use of notched samples has several advantages over the Nakajima test. Notched samples are less expensive to prepare and can be tested using standard tensile equipment, making this method more suitable for routine quality control purposes as well as research and development activities for new materials. Additionally, samples do not have any contact with the tools in the gauge section, and the sample could be heated easily with the traditional heating method used for dog bone samples.

The forementioned alternative approach involves creating a notch in the sheet metal sample. This notch changes the triaxiality of the tensile loading condition, inducing different strain conditions depending on the geometry of the notch. The strain at which the failure occurs is then used to determine the formability limit [12,13]. As the sample is subjected to tensile loading, the use of notched samples is limited to define the left-hand side of the FLD.

In order to have the whole FLD representation, i.e., the left- and the right-hand sides of the diagram, some works have used a hybrid approach, combining notched samples and other types of standard testing. For example, Djavanroodi and Janbakhsh [14] obtained the FLD using a standard tensile test for the uniaxial strain path; two different types of notched specimens for strain states between the uniaxial tension and the plane strain condition; and a circular specimen for the biaxial condition using hydroforming (see Figure 1). In the work developed in [14], the onset of localized necking was identified by examining the strain distribution profiles near the necking region and the strain on the surface of the samples was estimated through circular grids that were printed on the samples before the deformation. In the opinion of the authors of this work, this approach based on a combination of notched and standard-shaped samples can be useful for the FLD definition; however, the absence of DIC in the analysis reduces the accuracy since the onset and evolution of the crack during the test are not captured, and the analysis just focused on the results obtained at the end of the test. In addition, the circular grids approach is not suitable for samples with a small gauge length like the notched samples.

Recently, Kohl and Merklein [12] used a similar approach to determine the FLD to that of Djavanroodi and Janbakhsh [14], though this work used DIC to capture the surface strain. When determining the onset of necking, the authors used the so-called position-dependent method, which is a methodology designed for Nakajima samples as per the EN ISO 12004-2 standard [15]. In the opinion of the authors of this work, as will be shown later in this publication, this approach is not suitable for samples with a small gauge length, leading to some level of inaccuracy in the determination of the onset of necking.

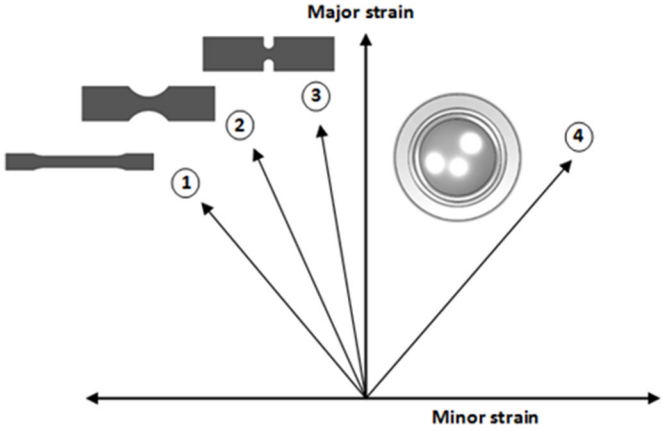

Figure 1. Different types of specimens representing the linear strain paths for (1) uniaxial tension, (2) intermediate tension, (3) near plane strain, and (4) biaxial tension [14].

The aim of the work presented here is to investigate the implementation of the notched samples approach as an alternative to the Nakajima testing for the left-hand side of the FLD using DIC to estimate the strain on the surface of the samples. Different to previous works, a new methodology for the strain limit definition, referred to as the time-dependent method, will be proposed. Results from this novel approach have been compared with the position-dependent method of the standard EN ISO 12004-2. Results from both methods have been also assessed against traditional Nakajima testing.

2. Methodology

In this work, a hybrid approach was used for the FLD determination. A standard tensile sample and two notched samples were used to identify the left-hand side forming limits. For the right-hand side, a biaxial sample from the Nakajima test was used.

Based on the literature review, the notched sample design will be selected for the targeted strain ratio. Then, the identified notched samples will be tested using DIC and the onset of the necking curve will be generated through the two previously mentioned approaches (position-dependent and time-dependent). To develop a full FLD curve, a damage equation was utilized to fit the generated FLC points. Finally, in parallel, a full Nakajima test was conducted to evaluate the performance of notched samples.

3. Experimental Work

AA6016-T4 material with a thickness of 2.5 mm was used in this analysis. The experimental work included the Nakajima test and notched tensile tests at room temperature to determine the failure limit of the material.

3.1. Nakajima Test

Based on the EN ISO 12004-2 standard, five different geometries were selected and cut using EDM to represent the FLD. The chosen specimens for the tests had the following widths: 40 mm, 80 mm, 100 mm, 120 mm, and 160 mm. The samples were sprayed with spackle patterns and the tests were conducted on a Zwick BUP 1000 Sheet Metal Testing machine. Tests were performed using a speed of 1.5 mm/s for the punch.

The FLC data was calculated using the ARAMIS software by defining section planes perpendicular to the crack orientation. Typically, three parallel sections should be selected to obtain the major and minor strain distributions along the length of the line of analysis. For the sake of simplicity, Figure 2 shows only one of those curves. Then, the software calculates an FLC point based on an inverse parabola fitting. The strain limit is considered the highest strain obtained from the bell-shaped curve. This approach is referred to as the position-dependent method and will be discussed in more detail in the next section.

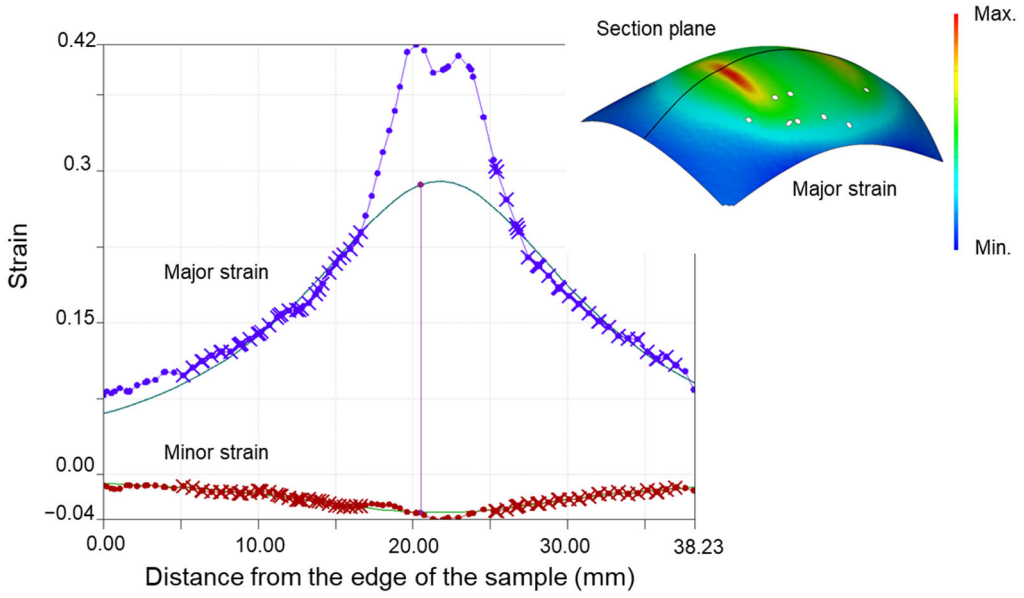

Figure 2. Evaluation of the inverse best-fit parabola on the "bell-shaped curve".

Figure 3 shows the generated FLD of the AA6061-T4 material obtained through the Nakajima testing using the position-dependent method for the strain limit definition, as per the EN ISO 12004-2 standard.

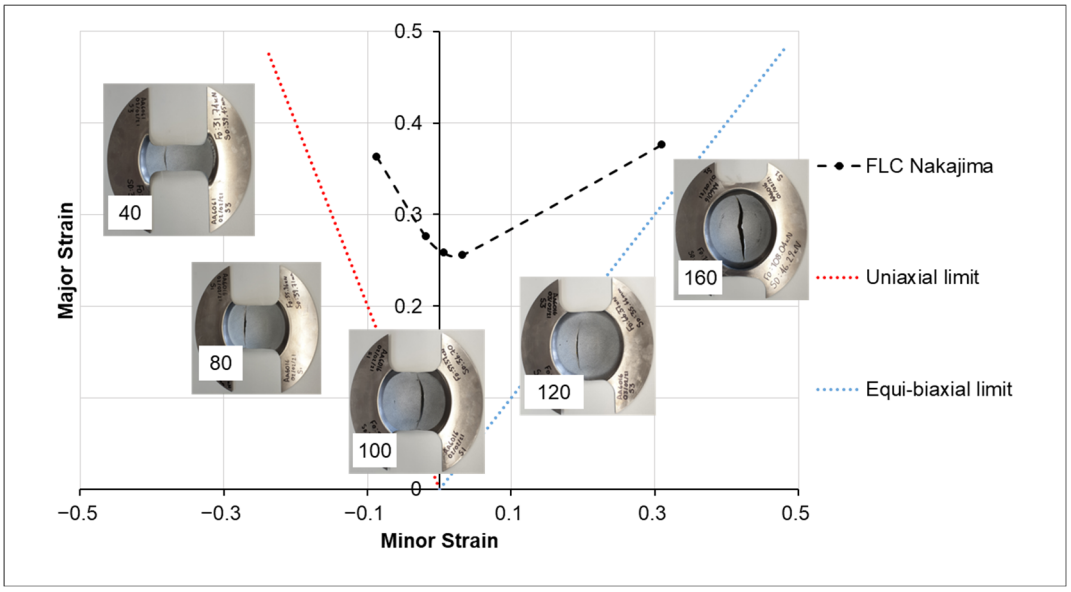

Figure 3. Measured FLD for AA6016-T4 using Nakajima test.

3.2. Tensile and Notched Tests

To develop the left-hand side of the FLD, the uniaxial tensile sample was selected to target a strain ratio of 0.5. For the notched samples, two samples were selected for a strain ratio of −0.25 and 0 [16]. The tensile sample and the two notched samples (that are referred to as intermediate-notched and plane-notched later in the text) were cut using EDM and then sprayed with the spackle pattern. Afterwards, samples were tested at a Zwick 250 universal testing machine at room temperature imposing a strain rate of 0.001/s (defined for a nominal gauge length of 15 mm). After testing, strains in the gauge length were estimated using the DIC technique implemented in the ARAMIS software, as described below. Samples were deformed until fracture, as the reader can see in Figure 4.

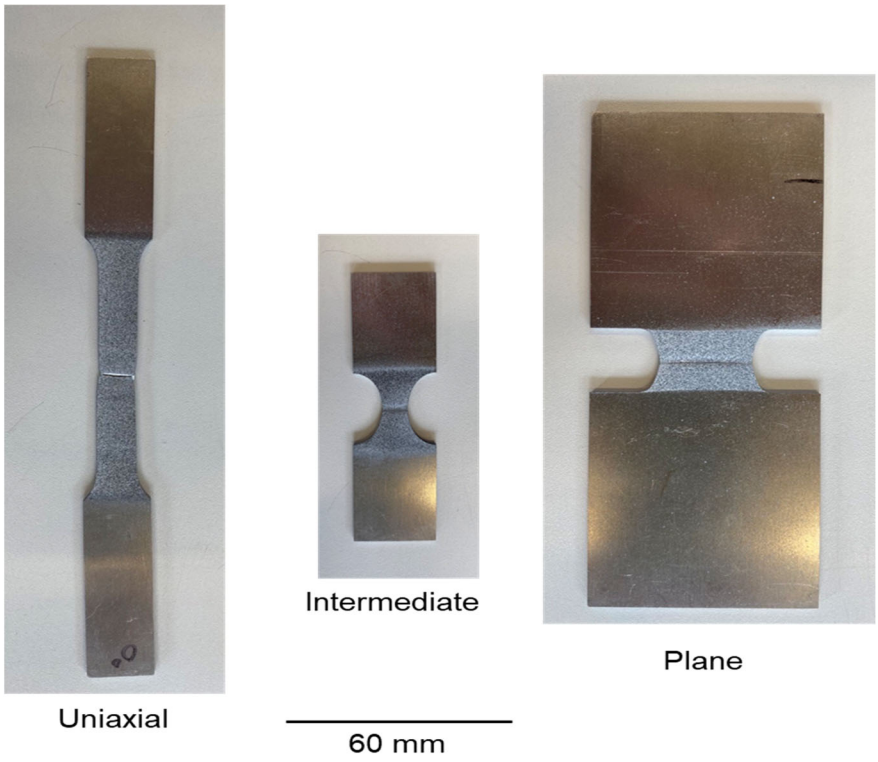

Figure 4. Uniaxial and notched samples tested until fracture.

4. Results and Discussions

For the notched samples, the images of the gauge length obtained during the test were imported to the GOM Correlate software to analyse the strains on the surface. Before any strain limit estimation, two key aspects were initially investigated through the DIC approach.

The first aspect is referred to as the crack location. As the reader can see in Figure 5, the two samples failed at the centre of the sample. This validates the notched samples approach as correct, due to the failure happening where the targeted strain ratio between major and minor strains is taking place and not in other areas of the gauge length where a different strain condition occurs. For instance, in the case of the plane-notched sample, the plane strain condition is achieved in the centre of the gauge length, with the strain ratio reaching there almost zero value, while at the edge of the notch, the strain condition becomes close to uniaxial, with the strain ratio taking a value close to -0.5. Having a crack in the centre of the sample guarantees that the material failed at the plane strain condition, which was the targeted condition; the same phenomenon was observed for the intermediate-notched sample. As a consequence of this, the strain estimated from the area of fracture in both notched samples represents the strain limit for the targeted strain ratio.

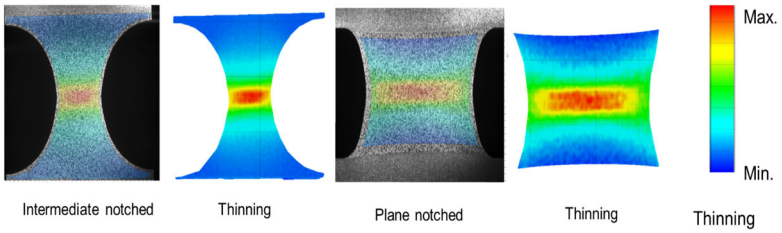

Figure 5. Thinning location for the notched samples at one frame before fracture.

The conditions above cannot always be guaranteed when working with the Nakajima tests due to friction. Indeed, if for any reason there is an increase in the coefficient of friction

in comparison to the targeted value in the standard, there is a risk for the crack to shift away from the centre of the sample [17]. This displacement of the crack will lead to inaccuracy in the analysis of the failure limits. For that reason, as specified in the standard, Nakajima tests should be rejected if the fracture occurs within a distance higher than 15% of the punch diameter away from the apex of the dome [15]. In comparison with the notched samples, no friction is introduced to the gauge section during the test. Therefore, better reliability can be achieved using notched samples compared to the Nakajima test. Figure 6 compares the results of the notched sample with those obtained with the Nakajima sample.

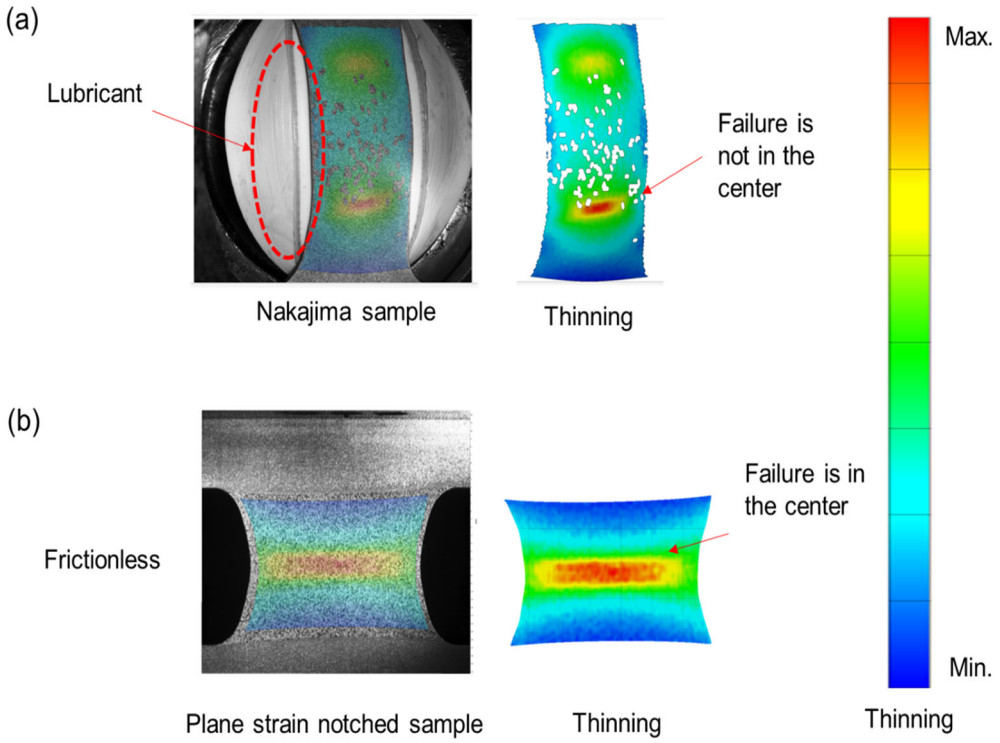

Figure 6. Effect of friction on the thinning location (**a**) Nakajima sample, and (**b**) notched sample.

The second aspect that was analysed through the DIC data is related to the strain path in the FLD followed by the major and minor strains developed at the cracked area during the duration of the test. A linear path in the FLD would guarantee a constant ratio between major and minor strains, i.e., the same strain condition during the whole duration of the test in the area where failure happens (centre of the gauge length).

Figure 7 shows the strain ratios measured through DIC for the tensile and the notched samples at the point of maximum major strain. As the reader can observe, all three samples showed a constant strain ratio during the duration of the test. For the plane-notched sample, a strain ratio of -0.1 was found. This value can be considered a good representation of the plane strain condition, as it is close enough to the targeted zero value. For the intermediate-notched sample, a strain ratio of -0.22 was measured. Finally, a strain ratio of -0.4 was estimated for the tensile sample (deviations from the -0.5 value are due to the material anisotropy that slightly drifted the strain ratio). These results validate the assumption that the notched samples approach can cover the left-hand side of the FLD successfully and can maintain the targeted strain ratio during the whole test.

Figure 8 highlights the strain path for the notched samples (intermediate) and the Nakajima sample with a similar strain ratio. It can be observed that the line reflecting the strain path from the notched sample is straighter when compared to the one obtained from the Nakajima sample. This as well confirms that the notched sample approach has higher accuracy compared to the Nakajima test regarding the stability of the strain ratio during the whole test. The obtained FLD points are affected by the linearity of the strain path [18,19].

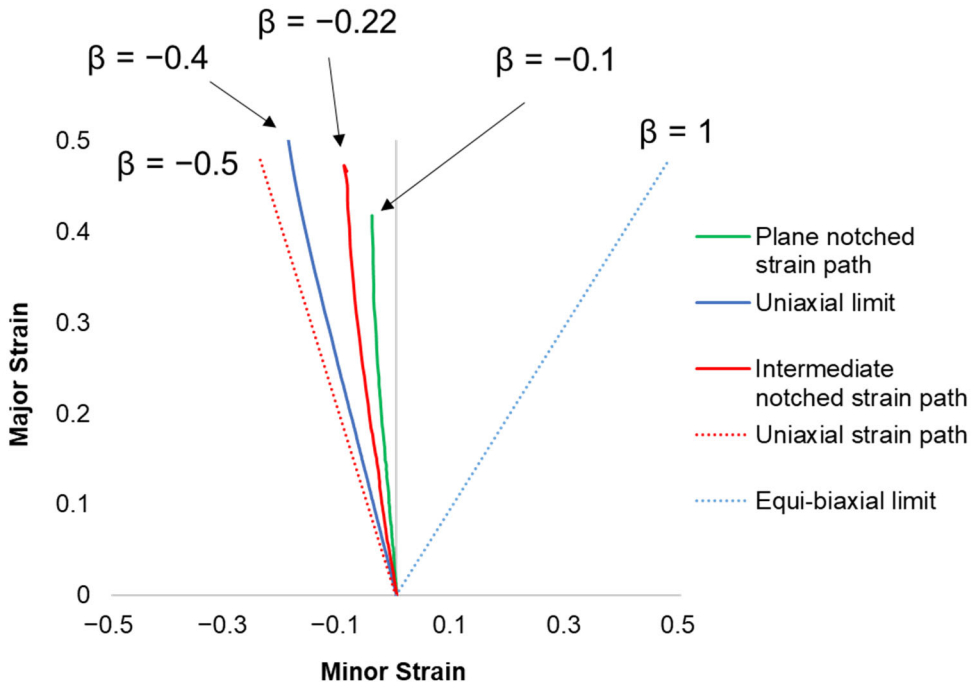

Figure 7. Strain path for one element at the centre on the maximum thinning for the three samples.

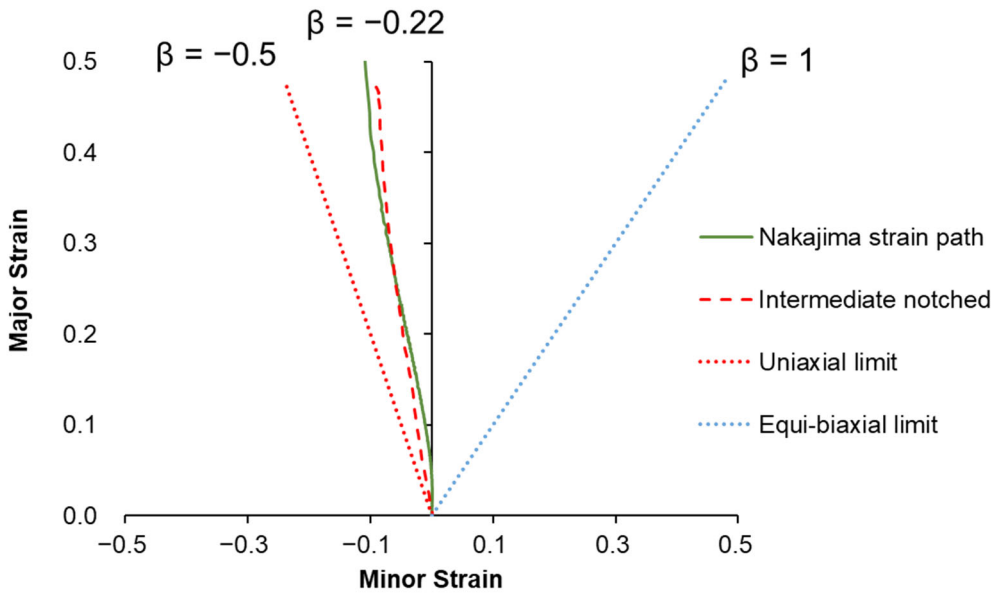

Figure 8. Strain path for notched sample and Nakajima sample at B = −0.22.

In this section of the paper, the authors demonstrated the validation of the notched samples approach, observing the correct location of the failure and the strain ratio value during the tests. In the next sections, two methodologies will be analysed in order to define the onset of necking, as well as to estimate the value of the strain limit.

4.1. Position-Dependent Method (Inverse Best-Fit Parabola)

The determination of the strain limit via the position-dependent method is based on the last captured image frame before fracture. The distribution of the major strain along the section obtained, based on a perpendicular plane to the fracture on the sample, is used in this methodology.

The first step of the position-dependent method consists of defining the interpolation window for the inverse parabola fitting that will be performed in the second step. These boundaries for the curve fitting are obtained based on a second derivative of the major strain along the distance of the section. Based on the standard, using three points for the calculation of the second derivative of the strain data is considered the second derivative without a filter. Also as per the standard, a filtered curve (smoothed) is obtained by using five points to calculate the second derivative. Once the second derivative is obtained (with and without filtering this magnitude), the two highest peaks of the calculated derivative define the inner boundaries. For the outer boundaries, an offset applied to the inner boundaries is calculated, proving the width of the fitting window. Once the fitting window is obtained, the major strain is fitted with an inverse parabola defined by Equation (1):

$$f(x) = \frac{1}{ax^2 + bx + c} \tag{1}$$

The forming limit is taken as the maximum value of the fitted parabola. Though calculations have been performed on the last frame before fracture, the obtained value refers to the strain limit for the onset of the necking. A similar approach is followed for the minor strain [15]. Figure 9 depicts the obtained results for the notched sample analysed in this work, showing a forming limit value of 0.46.

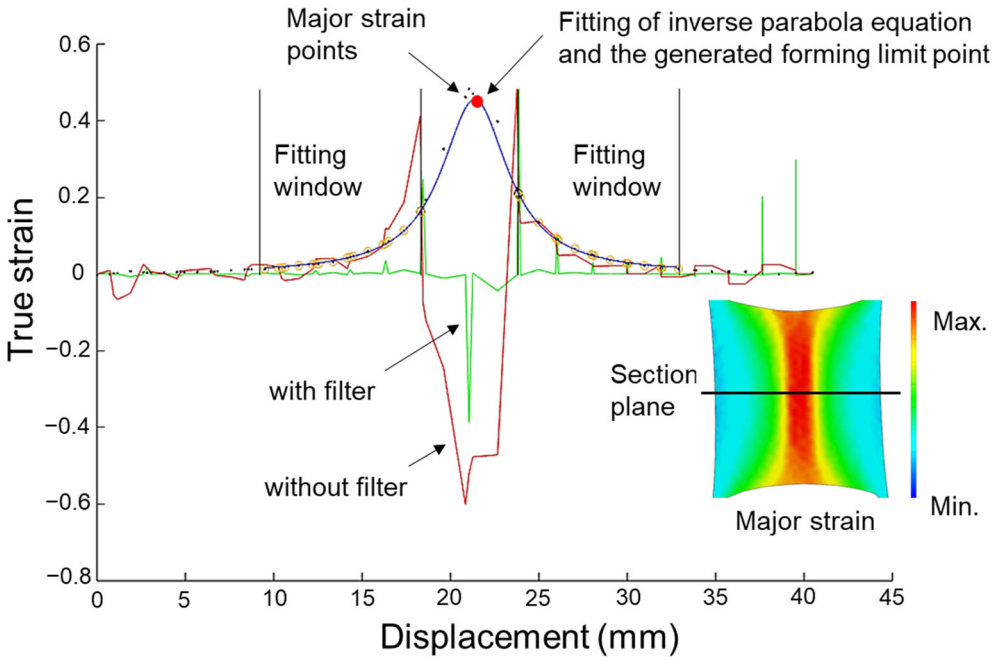

Figure 9. The development of FLD point for the notched sample through the position-dependent method.

4.2. Time-Dependent Method

The determination of the strain limit via the time-dependent approach is based on the temporal evaluation of the strain and the strain rate in a sequence of points located in the area of the fracture. As explained in the literature, the strain level of the points that are located inside the region of the plastic instability increases monotonically until the fracture, whereas points adjacent to the plastic instability region cease to strain and even undergo some elastic unloading immediately before failure [20,21].

Another example of the time-dependent approach can be found in the work of Martinez et al. [22]. Working with the Nakajima samples, the strain limit was defined based on a time-dependent method, based on the analysis of the major strain and the strain rate for a series of points (on either side of the crack) that are adjacent and also inside

the plastic instability area, as schematically explained in Figure 10. Two reference points were identified at the necking zone: the point at the boundary of the instability region (referred to as A) and the fracture point (referred to as B). Moving along the point selection (from inner to outer points), the boundary of the necking region (point A) is defined by the last point that ceases to strain and experiences a drop in strain rate just before the crack appears. Point B is identified as the point exhibiting the highest strain evolution. The onset of necking is considered to take place when point A exhibits a maximum in the strain rate magnitude. The strain at point B at that exact instant is considered the strain limit.

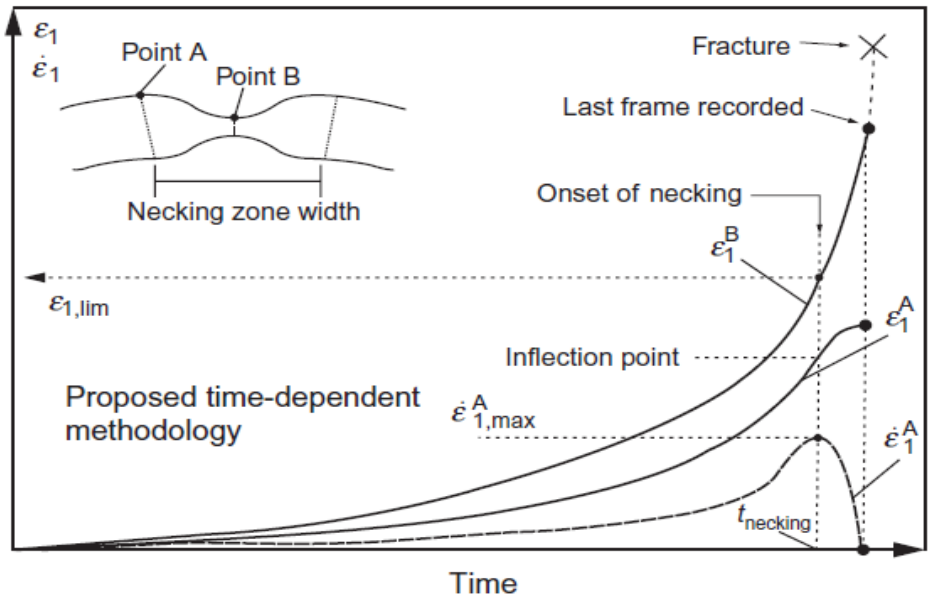

Figure 10. Schematic of the time-dependent methodology [22].

In the current work, a similar approach was followed for the notched samples (plane-notched and intermediate-notched), as well as for the tensile samples, analysing the DIC images obtained during the tests in order to define the strain limits for the different strain conditions.

Figure 11 presents the major strain distribution in the gauge length of the plane strain sample in the instant of the test close to the fracture. A section plane normal to the crack direction was constructed and a number of points were placed on that plane with a distance of 0.5 mm between them. The point with maximum strain was labelled as Point 1 (point B in Martinez et al.'s approach [22]). By analysing the evolution of the strain and strain rate during the time for all the selected points, the point at the boundary of the instability region (point A in Martinez et al.'s approach [22]) was found to be Point 5 (see Figure 12a–c), which has an offset of 2.5 mm from Point 1.

Analysing the strain rate of the selected points in Figure 12b, it can be observed that the instability of the strain rates starts at approximately a maximum strain of 0.21 in Point 1. From Figure 12c, the onset of necking time was detected based on the strain rate evolution of Point 5. A drop in the strain rate values can be observed. The maximum strain at the onset of necking time was 0.27 in Point 1. Figure 13 shows the DIC images for the major strain at the different identified phases.

Analysis of the intermediate-notched sample was performed using the same approach. Figure 14 presents the constructed section plane and the facet points on the gauge length of the sample. A 0.25 mm offset between the points was selected. As in the previous case, Point 1 was identified as the material point showing the maximum strain, and Point 5 was identified as the point at the boundary of the instability region, in this case, 1.5 mm away from Point 1. The onset of necking was detected and a maximum strain of 0.34 was found for that instant.

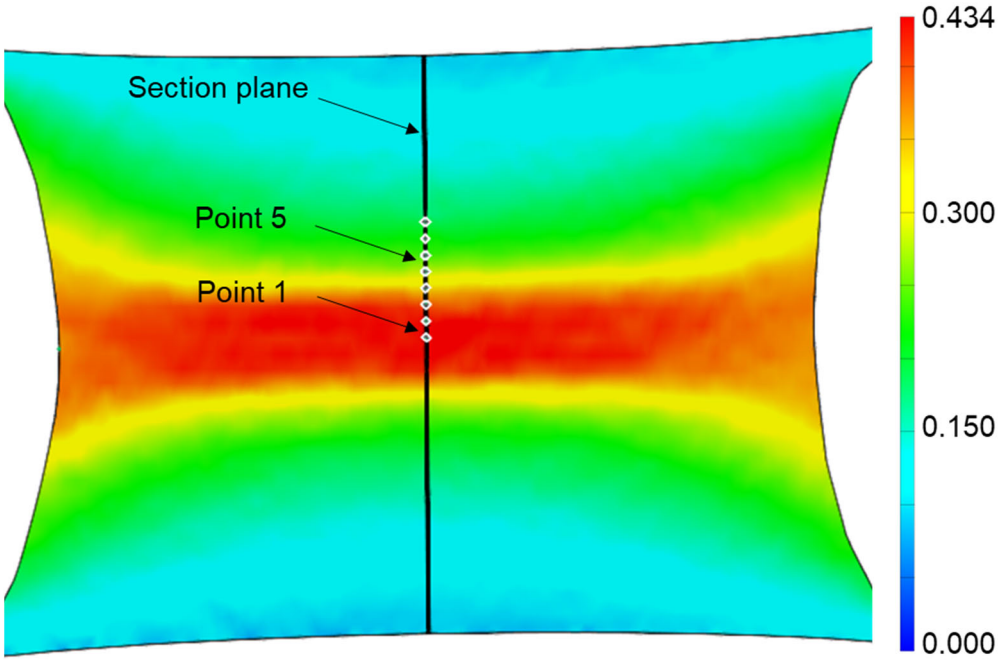

Figure 11. Major strain distribution on the plane-notched sample. A number of points were selected as part of the time-dependent analysis for the strain limit determination.

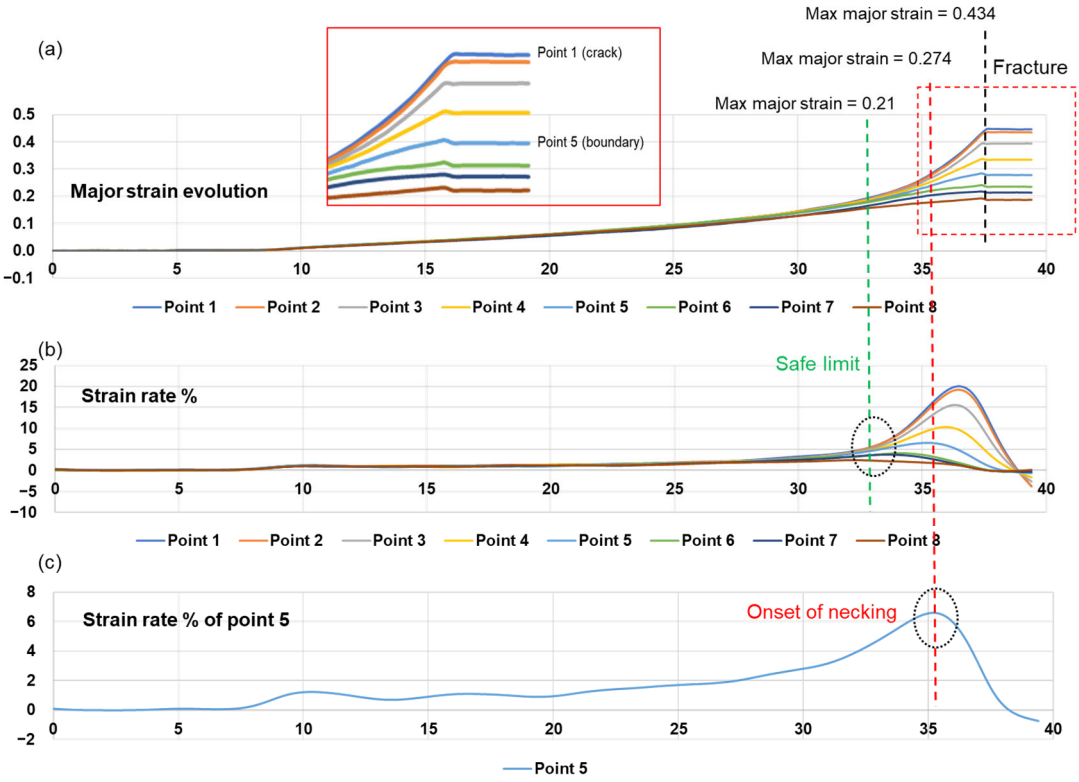

Figure 12. The analysis of the temporal evaluation of the strain data for the plane strain notched sample for (**a**) the major strain at different points, (**b**) the strain rate at different points, and (**c**) strain rate for the boundary point 5.

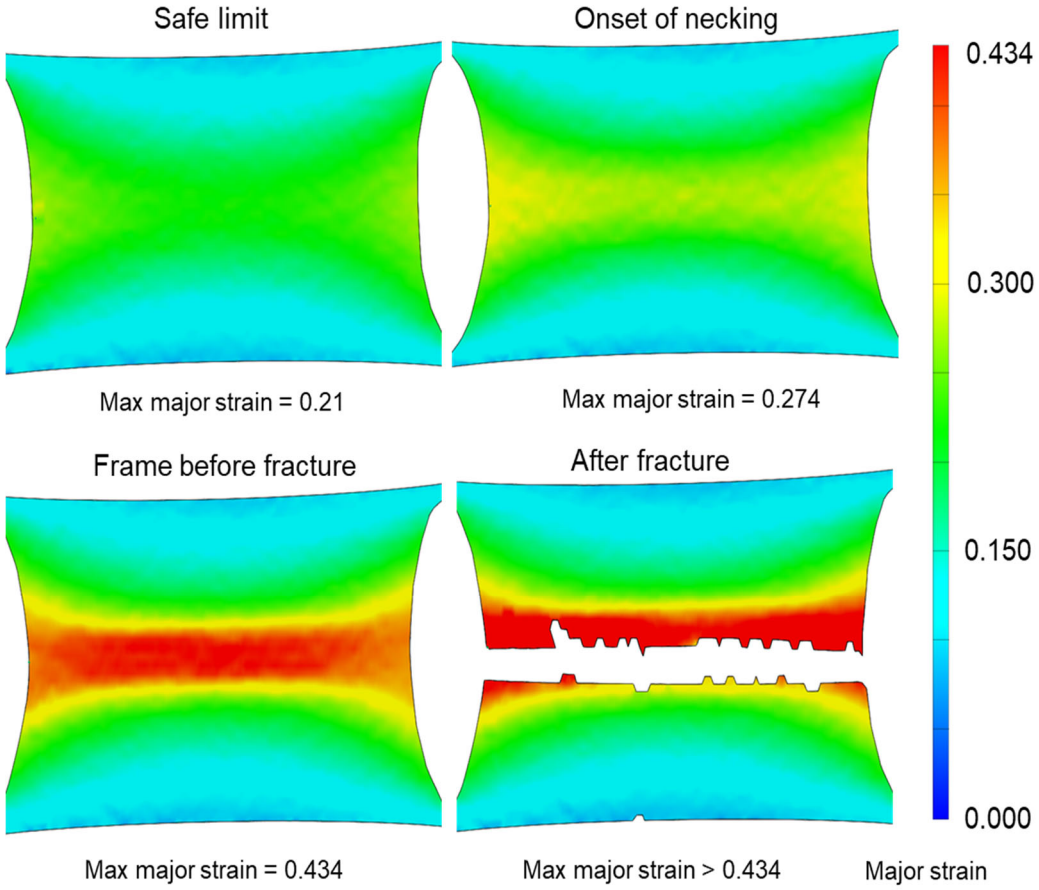

Figure 13. DIC images related to the evolution of the major strain for the notched-plane sample.

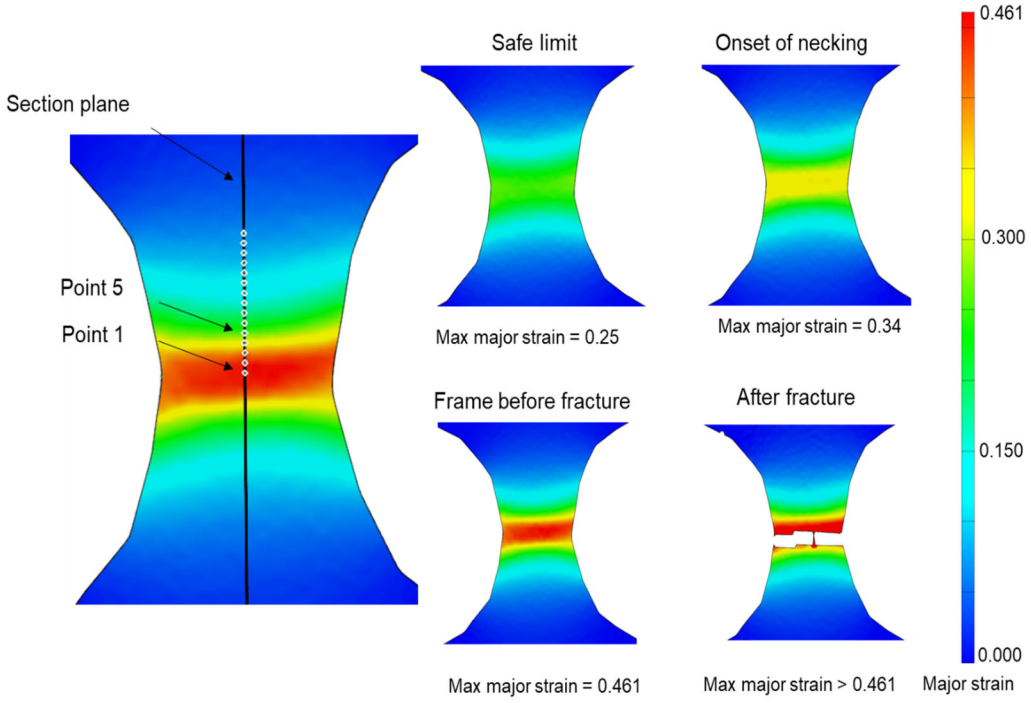

Figure 14. Major strain distribution on the intermediate-notched sample. A number of points are selected as part of the time-dependent analysis. In the figures on the right, the evolution of major strain for the intermediate-notched sample.

Similar to the notched samples, the uniaxial tensile sample was analysed, identifying different stages in the deformation process for this strain condition (Figure 15). The boundary limit (Point 6) was found at a distance of 3 mm from Point 1. The forming limit for the uniaxial sample was identified as 0.37.

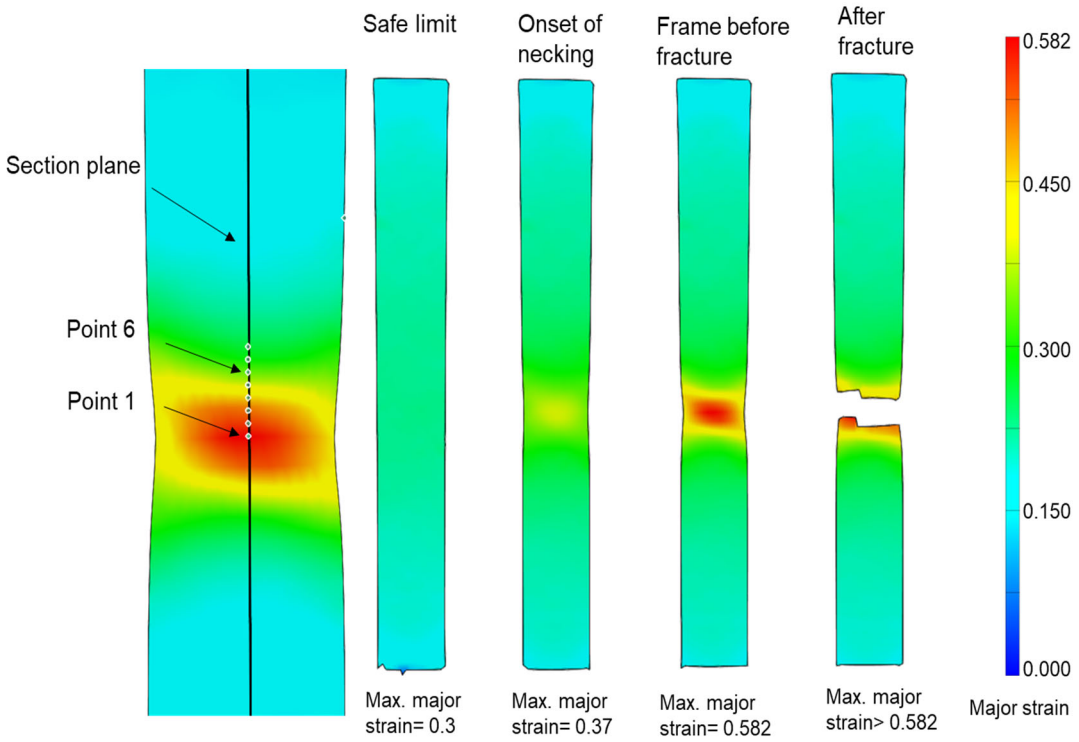

Figure 15. Data preparation for time-dependent analysis for the uniaxial sample on the major strain distribution and the evolution of major strain for the uniaxial sample.

Figure 16 depicts the points of the FLC identified through the analysis of the three samples. Though in the current work, only one sample was used to determine the forming limit, it is recommended to have a repetition of three samples and a minimum of two sections per sample.

Due to the limited FLC points obtained, Hu et al.'s [23] ductile damage model was used. In this model, the maximum shear stress is chosen and normalized by the equivalent stress to describe the influences of the shearing mechanism, while the stress triaxiality is selected to represent the effects of the tension mechanism [24].

Equation (1) presents the damage equation used to develop the whole curve of the FLC. Parameters of Equation (1) were estimated based on the data from the tensile, notched samples and the biaxial sample from the Nakajima test.

$$D = \frac{1}{C_3}\int_0^{\bar{\varepsilon}_f}\left[\left(\frac{2\bar{\tau}_{max}}{\bar{\sigma}}\right)^{C_1} + \left(\eta - \frac{1}{3}\right)\right]^{C_2} d\bar{\varepsilon}_p \quad (2)$$

where D is the damage parameter; $\bar{\varepsilon}_f$ is the effective strain at failure; $\bar{\sigma}$ is the effective stress; $\bar{\tau}_{max}$ is the maximum shear stress; η is the stress triaxiality; $d\bar{\varepsilon}_p$ is the incremental effective plastic strain; C_1, C_2, and C_3 are material constants.

Figure 17 presents the developed FLC after having fitted Equation (1) with the data of the tensile and notched tests. A good agreement exists between the developed FLC and the curve fitted to the experimental points of the Nakajima test.

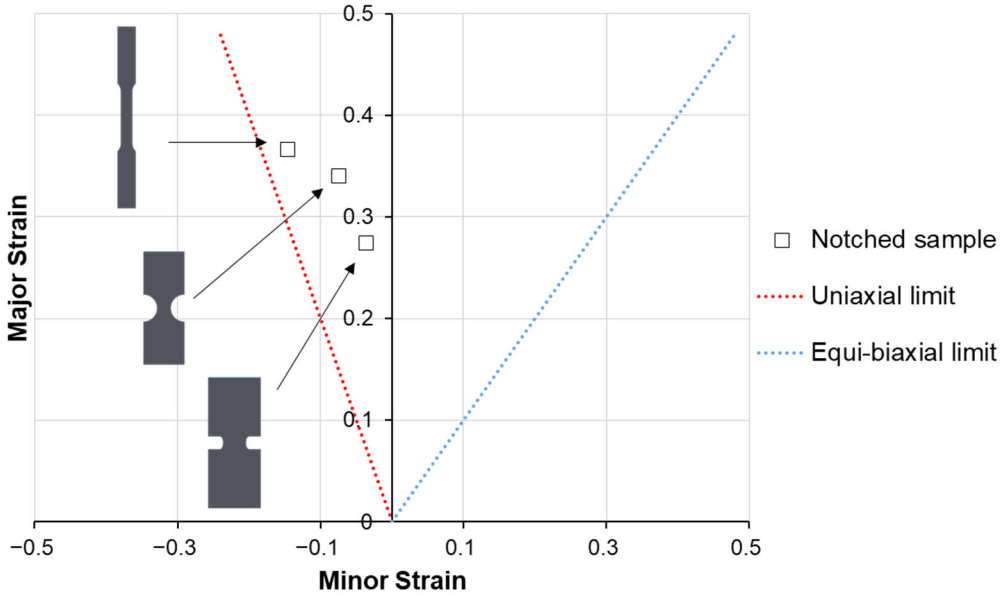

Figure 16. The forming limits points obtained from notched sample approach.

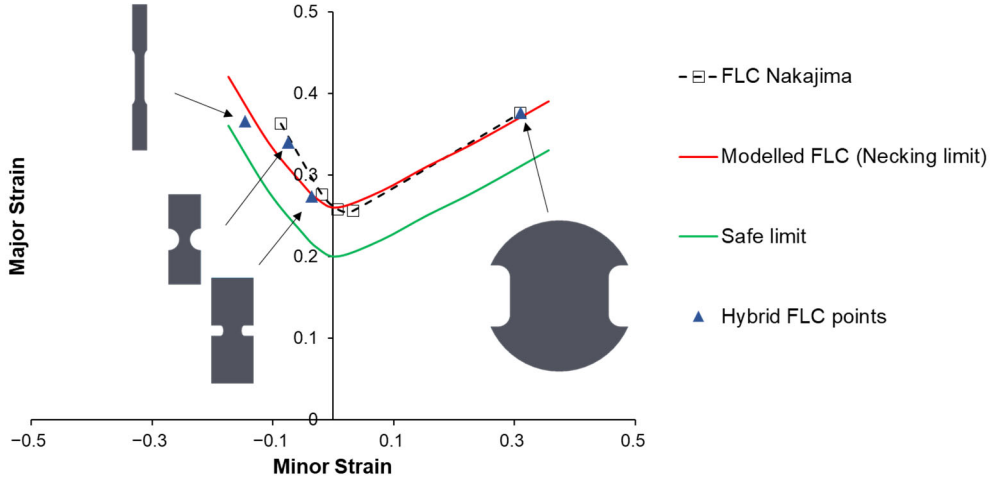

Figure 17. The developed FLD for AA6016-T4 using the hybrid approach.

From Figure 17, it can also be noticed that the Nakajima test results for the uniaxial case do not accurately match the strain limit obtained from the tensile sample: the strain ratio coming from the Nakajima tests for the uniaxial condition was −0.22, whereas the tensile sample yield a value of −0.4. The developed hybrid approach using the tensile sample provides more accuracy to the FLC obtained via curve fitting.

With the prediction of the FLC proposed in this work, an accurate value for the plane strain forming limit can be obtained by considering a null value for the minor strain.

Finally, using the data captured from DIC, an approximate characterization for the safe and risk regions have also been developed, which can be significantly helpful for simulation activities. It should be said that in the current approach followed by the industry, the safe zone is defined by an approximate offset from the FLC. This offset value varies depending on the source of the FLC. The proposed approach provides a more accurate definition of the safe region.

5. Conclusions

In this study, a hybrid approach to identify the forming limits of AA6016-T4 was investigated. This hybrid approach included the use of the notched samples for the

left-hand side of the FLD and the biaxial Nakajima test for the right-hand side. The time-dependent method was used to obtain the onset of necking strain. A good agreement was found between the proposed hybrid approach and the standard Nakajima test. The following points have been concluded:

- It has been confirmed that notched can be used to target plane strain conditions; however, a 10% error is expected in the achieved strain ratio as the ratio might shift slightly towards the negative minor strain. In addition, using notched samples was found to be significantly beneficial in terms of cost, accuracy, and time. The geometry of the notch in the gauge area is also very flexible to adapt for different lengths and the introduction of temperature in the testing can be implemented as it is performed in standard tensile tests;
- Although the position-dependent method applies a parabola fitting technique to define the limit strains rather than using the actual physical measurement, it was observed that this method can provide a good estimation for the necking limits of the material when using the standard Nakajima samples; however, it is not designed for samples with small gauge lengths as it might overestimate the onset of necking;
- The accuracy of the time-dependent method depends on the accuracy of strain measurements, especially the number of captured frames-per-second, as the method depends on the evolution of strain rate and the definition of the boundary limit, which depends on the gauge length;
- It was found that DIC applied to notched samples can capture the different phases of deformation, i.e., safe limit, the onset of necking, and fracture. This provided valuable information on both the safe and risk zones of the FLD; in addition, it can be used to calibrate accurate damage models with support simulation activities.

This paper presents a new hybrid approach to determine the FLC experimentally using notched samples; however, further research with different materials is necessary to verify this methodology. Furthermore, the reliability of this approach under different temperatures and different strain rates needs to be investigated.

Author Contributions: Conceptualization, A.E.; Methodology, A.E.; Validation, A.E. and D.G.; Investigation, A.E., D.G. and E.Y.; Data curation, A.E.; Writing—original draft, A.E., D.G. and E.Y.; Writing—review & editing, D.G. and E.Y.; Supervision, D.G. and E.Y. All authors have read and agreed to the published version of the manuscript.

Funding: This research received no external funding.

Data Availability Statement: Data sharing not applicable.

Conflicts of Interest: The authors declare no conflict of interest.

References

1. Marciniak, Z.; Hu, J.; Duncan, J. 5–Load instability and tearing. In *Mechanics of Sheet Metal Forming*, 2nd ed.; Marciniak, Z., Duncan, J.L., Hu, S.J., Eds.; Butterworth-Heinemann: Oxford, UK, 2002; pp. 61–81.
2. Dahan, Y.; Chastel, Y.; Duroux, P.; Wilsius, J.; Hein, P.; Massoni, E. Procedure for the experimental determination of a forming limit curve for usibor 1500 P. In Proceedings of the IDDRG 2007 International Conference Proceedings, Győr, Hungary, 21–23 May 2007.
3. Slota, J.; Jurčišin, M.; Spišák, E.; Tomáš, M.; Šiser, M. Experimental Flc Determination of High Strength Steel Sheet Metal. *Acta Metall. Slovaca* **2015**, *21*, 269–277. [CrossRef]
4. Keeler, S. Circular Grid System—A Valuable Aid for Evaluating Sheet Metal Formability. *SAE Tech. Pap.* **1968**, *77*, 371–379. [CrossRef]
5. Goodwin, G.M. Application of strain analysis to sheet metal forming in the press shop. *SAE Tech. Pap.* **1968**, *77*, 380–387. [CrossRef]
6. Sowerby, R.; Chu, E.; Duncan, J.L. Determination of large strains in metal forming. *J. Strain Anal. Eng. Des.* **1982**, *17*, 95–101. [CrossRef]
7. Tan, Z.; Melin, L.; Magnusson, C. Application of an image processing technique in strain measurement in sheet metal forming. *J. Mater. Process. Technol.* **1992**, *33*, 299–310. [CrossRef]

8. Vacher, P.; Haddad, A.; Arrieux, R. Determination of the forming limit diagrams using image analysis by the correlation method. *CIRP Ann. Manuf. Technol.* **1999**, *48*, 227–230. [CrossRef]
9. Wang, K.; Carsley, J.E.; He, B.; Li, J.; Zhang, L. Measuring forming limit strains with digital image correlation analysis. *J. Mater. Process. Technol.* **2014**, *214*, 1120–1130. [CrossRef]
10. Kasaei, M.M.; Oliveira, M.C. Influence of the contact with friction on the deformation behavior of advanced high strength steels in the Nakajima test. *J. Strain Anal. Eng. Des.* **2021**, *57*, 193–207. [CrossRef]
11. Reuther, F.; Lieber, T.; Heidrich, J.; Kräusel, V. Numerical Investigations on Thermal Forming Limit Testing with Local Inductive Heating for Hot Forming of AA7075. *Materials* **2021**, *14*, 1882. [CrossRef] [PubMed]
12. Kohl, D.; Merklein, M. Alternative characterization method for the failure behavior of sheet metals derived from Nakajima test. *IOP Conf. Ser. Mater. Sci. Eng.* **2021**, *1157*, 012046. [CrossRef]
13. Gruben, G.; Morin, D.; Langseth, M.; Hopperstad, O. Strain localization and ductile fracture in advanced high-strength steel sheets. *Eur. J. Mech. A/Solids* **2016**, *61*, 315–329. [CrossRef]
14. Djavanroodi, F.; Janbakhsh, M. Formability characterization of titanium alloy sheets. In *Titanium Alloys*; Jan, S., Waldemar, Z., Eds.; IntechOpen: Rijeka, Croatia, 2013; pp. 81–113.
15. EN ISO 12004-2:2008—Metallic Materials—Sheet and Strip—Determination of Forming-Limit Curves—Part 2: Determination of Forming-Limit Curves in the Laboratory (ISO 12004-2:2008). Available online: https://www.iso.org/standard/43621.html (accessed on 8 June 2023).
16. Achani, D.; Lademo, O.-G.; Engler, O.; Hopperstad, O.S. Evaluation of constitutive models for textured aluminium alloys using plane-strain tension and shear tests. *Int. J. Mater. Form.* **2011**, *4*, 227–241. [CrossRef]
17. Mohamed, M.; Farouk, M.; Elsayed, A.; Shazly, M.; Hegazy, A.A. An investigation of friction effect on formability of AA 6061-T4 sheet during cold forming condition. In Proceedings of the 20th International Esaform Conference On Material Forming: Esaform 2017, Dublin, Ireland, 26–28 April 2017.
18. Gutiérrez, D.; Lara, A.; Casellas, D.; Prado, J. Effect of Strain Paths on Formability Evaluation of TRIP Steels. *Adv. Mater. Res.* **2010**, *89*, 214–219. [CrossRef]
19. He, J.; Zeng, D.; Zhu, X.; Xia, Z.C.; Li, S. Effect of nonlinear strain paths on forming limits under isotropic and anisotropic hardening. *Int. J. Solids Struct.* **2014**, *51*, 402–415. [CrossRef]
20. Centeno, G.; Martínez-Donaire, A.J.; Morales-Palma, D.; Vallellano, C.; Silva, M.B.; Martins, P.A.F. 1–Novel experimental techniques for the determination of the forming limits at necking and fracture. In *Materials Forming and Machining*; Davim, J.P., Ed.; Woodhead Publishing: Cambridge, UK, 2015; pp. 1–24.
21. Silva, M.B.; Martínez-Donaire, A.J.; Centeno, G.; Morales-Palma, D.; Vallellano, C.; Martins, P.A.F. Recent Approaches for the Determination of Forming Limits by Necking and Fracture in Sheet Metal Forming. *Procedia Eng.* **2015**, *132*, 342–349. [CrossRef]
22. Martínez-Donaire, A.J.; García-Lomas, F.J.; Vallellano, C. New approaches to detect the onset of localised necking in sheets under through-thickness strain gradients. *Mater. Des.* **2014**, *57*, 135–145. [CrossRef]
23. Hu, Q.; Zhang, F.; Li, X.; Chen, J. Overview on the Prediction Models for Sheet Metal Forming Failure: Necking and Ductile Fracture. *Acta Mech. Solida Sin.* **2018**, *31*, 259–289. [CrossRef]
24. Nouira, M.; Oliveira, M.C.; Khalfallah, A.; Alves, J.L.; Menezes, L.F. Comparative fracture prediction study for two materials under a wide range of stress states using seven uncoupled models. *Eng. Fract. Mech.* **2023**, *279*, 108952. [CrossRef]